Finite-difference staggered-grid modelling in 3 dimensions

Peter M Manning

ABSTRACT

The elastic finite-difference modelling method, which uses staggered grid displacement positions and which has proved effective in 2 dimensions, has been extended for use in 3 dimensions. The geometry of the grid positions is shown from selected viewpoints. For an isotropic, homogeneous medium, four types of finite-difference energy sources are examined, and the propagating wavefronts expected from them are shown. The accuracy of one of the energy source models is verified by comparison with the double-couple solution from known theoretical results.

INTRODUCTION

The author has developed a versatile set of two-dimensional elastic, isotropic, finite-difference modeling programs, which depend on the staggered-grid for their success, and which are described in his thesis (Manning 2007). The thesis shows how effective the staggered-grid is for controlling high frequency noise while allowing accurate reproduction of body and surface wave propagation. These advantages can also be expected when propagating waves in 3 dimensions because the same geometric relationships apply. Correction factors were a large part of the Manning thesis, but they have not yet been applied to any models in 3 dimensions.

It is not immediately obvious that the staggered-grid is a valid construction for all 3 dimensions of a model space, but it may be seen in the structure known as 'face centered cubic' from crystallography. Guo Tao and his group from the Chinese National Petroleum University have been using the concept since 2002 to model borehole logging instrument responses.

Finite-difference models in 3 dimensions have always been possible, but only recently do they appear to have significant practical application as computing power has increased. This is especially true as computer clusters have become larger and more readily available. The code here has not yet been used successfully on a cluster, but has been designed for that possibility in the future.

THEORY

The starting point for all wave propagation models is the vector wave equation. The finite-difference solution given here depends upon the representation in Cartesian coordinates, and is derived from the three simultaneous equations for displacement in an isotropic elastic medium

$$\left(\lambda + 2\mu\right)\frac{\partial^2 U_x}{\partial x^2} + \left(\lambda + \mu\right)\left[\frac{\partial^2 U_y}{\partial x \partial y} + \frac{\partial^2 U_z}{\partial x \partial z}\right] + \mu\left[\frac{\partial^2 U_x}{\partial y^2} + \frac{\partial^2 U_x}{\partial z^2}\right] = \rho\frac{\partial^2 U_x}{\partial t^2}, \qquad (1)$$

$$\left(\lambda + 2\mu\right)\frac{\partial^2 U_y}{\partial y^2} + \left(\lambda + \mu\right)\left[\frac{\partial^2 U_x}{\partial x \partial y} + \frac{\partial^2 U_z}{\partial y \partial z}\right] + \mu\left[\frac{\partial^2 U_y}{\partial x^2} + \frac{\partial^2 U_y}{\partial z^2}\right] = \rho\frac{\partial^2 U_y}{\partial t^2}, \qquad (2)$$

$$\left(\lambda + 2\mu\right)\frac{\partial^2 U_z}{\partial z^2} + \left(\lambda + \mu\right)\left[\frac{\partial^2 U_x}{\partial x \partial z} + \frac{\partial^2 U_y}{\partial y \partial z}\right] + \mu\left[\frac{\partial^2 U_z}{\partial x^2} + \frac{\partial^2 U_z}{\partial y^2}\right] = \rho\frac{\partial^2 U_z}{\partial t^2}, \qquad (3)$$

where U_x, U_y, and U_z are displacements, and λ and μ are the Lame parameters.

All of the terms here take the same form as those used for modelling in two dimensions. In fact, the equations for the two dimensions x and z may be obtained by dropping all the terms with a y component, and which vary with y. This eliminates the second equation and removes two terms from each of the other two equations.

The finite-difference solution is obtained by a time-stepping procedure, where the three components of the displacement at a given time are plugged into finite-difference versions of the second derivatives, and the properly weighted sums are used to calculate the accelerating force. All this is done on the left side of the equations. On the right side the second derivative is decomposed, and by using the past displacement and momentum, displacements are computed for the succeeding time step.

IMPLEMENTATION

The staggered grid

The key to effective finite-difference modelling is the staggered grid, and this applies to 3 dimensional as well as 2 dimensional cases. It is a bit surprising to find that every displacement component is located on two of the 3 planes oriented in the directions of the axes, and each plane includes, in staggered positions, the perpendicular displacements required to compute the necessary second derivatives.

The staggered grid used must take a form similar to that shown in Figures 1 and 2. The Figures show the same 3 dimensional grid, but each is observed from an angle where particular planes may be seen within which the displacements are staggered from each other. Figure 1 shows the flat XY planes with the displacements coded red for X displacement, and blue for Y displacement. Figure 2 shows the vertical YZ planes, with blue for Y displacement and black for Z displacement. The vertical XZ planes may also be shown to have the same relationships.

EXAMPLES

Energy source models

Models have been initiated with energy in very limited spatial configurations, but extended over time to control frequency content. This is the most convenient method, but does not provide exact control of the waveform. The sources have been configured in four forms.

The most conventional source is the isotropic explosion of Figure 3a, which simulates a dynamite blast. The energy is initiated in 3 opposed vector pairs, in the X, Y and Z directions, coloured red, blue and black. This is a direct source of pressure waves only.

The next source is the 'double couple' shown in Figure 3b. This is the source described by Aki and Richards (1980, section 4.3), and which seismologists have shown to be a very successful model of earthquake events. The horizontal (in this case X) couple can be considered as defining the strike/slip of the earthquake event, and the opposing couple may be considered as a requirement to make the event non-rotational. The radiation from this source is dependent on the direction to the observer compared to the direction of the slip, and it will generate shear waves as well as pressure waves.

A source which is similar to the 'double couple' is the 'squeeze bulge' source shown in Figure 4a. This has a signature similar to the 'double couple' but rotated by 45 degrees. A finite-difference slip simulation at an arbitrary angle might require a combination of these two sources.

The last source used is the 'Z-rupture' shown in Figure 4b, represented in the Z direction by a single opposed pair. This may provide the best simulation of the radiation generated from pressure fracturing events. Because the displacements from this source are not spherically symmetric, it will generate shear as well as pressure waves. The radiation patterns from this source will be symmetric about the axis of the displacement.

Wavefront snapshots from energy sources

A snapshot from an explosive energy source is plotted in Figure 5. The display is a slice through the spherical wavefront and goes through the source point at the centre. The colours are the same as those used in Manning (2007, appendix F), and they are useful here because all displacements are within this plane. The colours show the radial symmetry which may be expected from an explosive source.

Figure 6 shows the wavefronts which have propagated from the 'double couple' energy source of Figure 3a. The plane of the display is through the source point, and also in the plane of the source vectors. The pressure wave is divided into four quadrants, with two quadrants on opposing sides having polarity opposite to those of the perpendicular quadrants. The nodes are aligned in the vertical and horizontal directions.

The shear waves generated from the same source time travel at half the speed, and have amplitudes more than 8 times as large (see the next section for the Aki/Richards theory). The wavefronts are very similar to the pressure waves, but are oriented at 45 degrees to them.

Figure 7 displays the same data as Figure 6, but with lower amplitude so the shear wavefront details may be seen.

Figure 8 shows the wavefronts from the 'squeeze/bulge' energy source. It is very similar to the plot of Figure 6, but rotated 45 degrees. The similarity of the two sources may be seen by dividing each vector into two components at 45 degrees from the original direction, and then summing the vectors which have the same resultant direction.

Figure 9 shows the wavefronts which have propagated from the 'Z-rupture' source of Figure 4b. The pressure wave is very similar to the 'explosive' source model, except that the amplitudes fade to zero in the horizontal directions. The shear waves are very similar to those from the 'squeeze/bulge' model, except the amplitude variation between the pressure and shear waves do not seem to be quite as large.

The Aki-Richards double couple model

The book written by Aki and Richards (1980) is a very widely used source for seismologists and other geophysicists. The 'double couple' model developed in the book has been very successfully used for interpreting recordings from seismic events, and it therefore must describe the nature of fault slippage accurately. The model provides analytic expressions for the wave fields generated from one of these events, and so the results may be compared with finite-difference results from similar sources.

The formulae from Aki and Richards for the far-field (part of 4.32 and 4.33 on page 81) were coded in Matlab and displayed with the same plotting methods used for the finite-difference codes. The results are shown in Figures 10 and 11.

The large difference in amplitudes of the pressure and shear waves are explained within equation 4.32, the far field portion of which is.

$$u(x,t) = \ldots + \frac{1}{4\pi\rho\alpha^3} A^{FP} \frac{1}{r} M_0\left(t - \frac{r}{\alpha}\right) + \frac{1}{4\pi\rho\beta^3} A^{FS} \frac{1}{r} M_0\left(t - \frac{r}{\beta}\right), \qquad 4)$$

where ρ is density, α is compressional velocity, β is shear velocity, the A's contain the spherical unit vectors from the equations in 4.33, r is the radial distance , M_0 is the time wavelet, and t is the time. Note the factors α and β, both cubed, in the denominators of the amplitude formulae for the pressure and shear waves. These pressure and shear velocities, with the assumed ratio of 2 to 1, bring the amplitude ratio to 8 to 1. The ratio is further increased by the smaller radial distance at the point where the shear wave exists.

The spatial wavelet in equation 4 is translated directly from a time wavelet (M_0), by use of the factors r/α and r/β. This shows in Figure 10 where the zero phase character of the original Ricker wavelet may be seen. Comparison with Figure 6 shows similarity in overall appearance but differences in the detailed wavelets.

A discrepancy of this nature was noted in Manning (2007, Appendix G), where it was found that the opposing couples of finite-difference sources in time seem to differentiate the time wavelet. A differentiated Ricker wavelet was therefore used within the Aki-Richards model, and the result is shown in Figure 11. This matches the finite-difference model results a little more closely.

CONCLUSIONS

Finite-difference models in three dimensions can make use of several types of realistic energy sources.

The double couple finite-difference energy source has an encouraging similarity to its theoretical equivalent.

FUTURE WORK

Vibroseis type energy sources need to be developed and tested.

Colour coded wavefield presentations must be improved so that slices through arbitrary volumes are meaningful.

REFERENCES

Aki, K., and Richards, P. G., 1980, Quantitative Seismology: W.H. Freeman and Co., first edn.
Manning, P. M., 2007, Techniques to enhance the accuracy and efficiency of finite-difference modeling for the propagation of elastic waves: PhD thesis

FIGURES
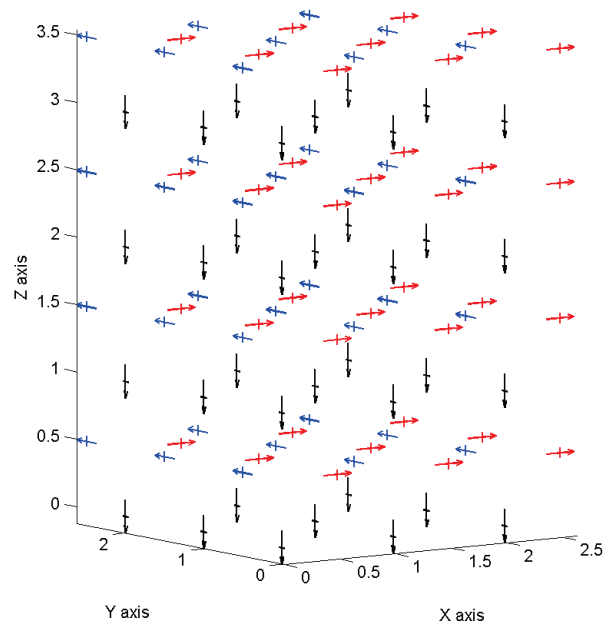
FIG.1. The staggered grid layout for 3D finite-difference modelling. X displacements are red, Y displacements are blue, and Z displacements are black. From this angle, the X and Y displacements may be seen to form a flat plane with the X's and Y's at staggered positions.
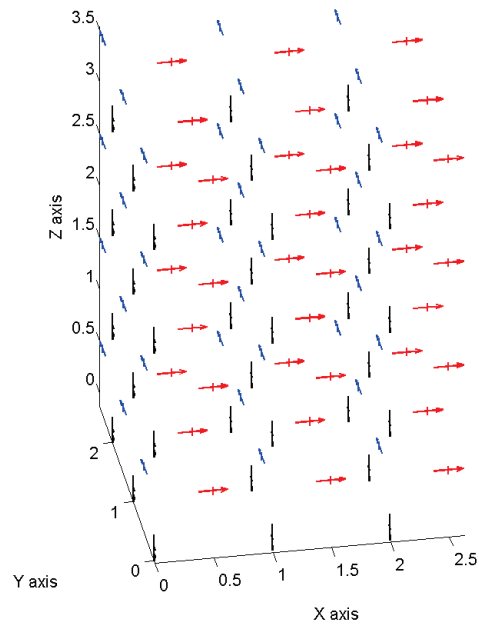
FIG.2. The same 3D staggered grid as the one depicted in Figure 1, with the same colour representation for displacements, but shown from a different angle. Here the Y and Z components (blue and black) can be seen to form vertical planes in which the two sets of displacements are staggered from each other.
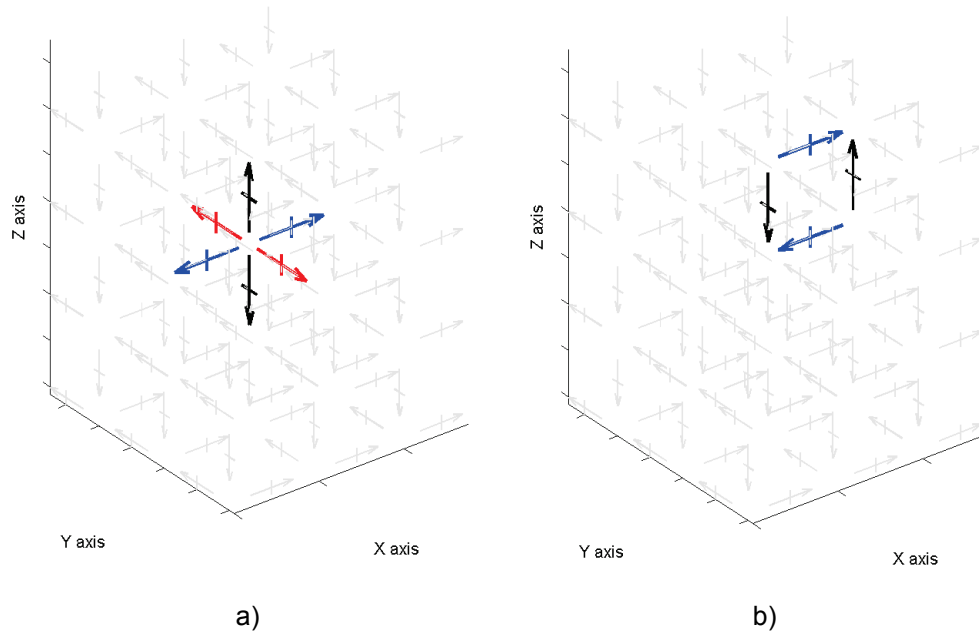

a)   b)

FIG.3. Two possible source types used to initiate finite-difference models. The 'explosive' source in a) simulates a dynamite blast. It expands in all directions and generates only pressure waves. The 'double couple' in b) simulates a strike/slip earthquake event. This is the source which is modelled in the book by Aki and Richards (1980).The displacements are blue in the X direction, red in the Y direction, and black in the Z direction.

a)   b)
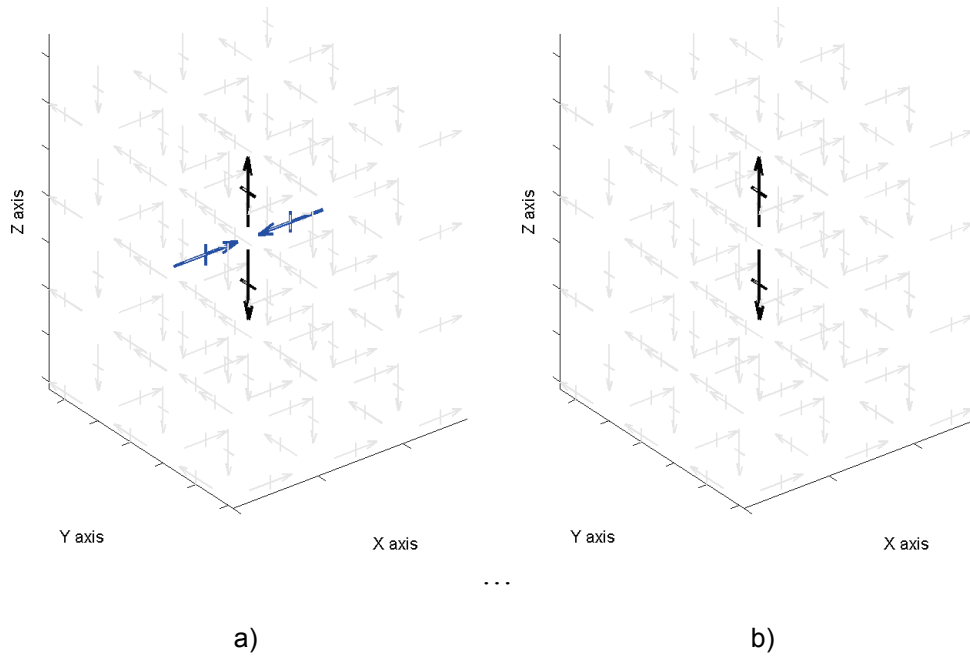
FIG. 4. The 'squeeze/bulge' in a) is closely related to the rotated 'double couple' in Figure 3a. Summing the vectors in pairs along axes rotated at 45 degrees will show this. The 'Z-rupture' in b) is a candidate to model the events associated with well fracturing operations. This is one of the couples mentioned in Aki and Richards. It is a component of the 'explosive' source, but since it is not spherically symmetric, it generates shear waves.
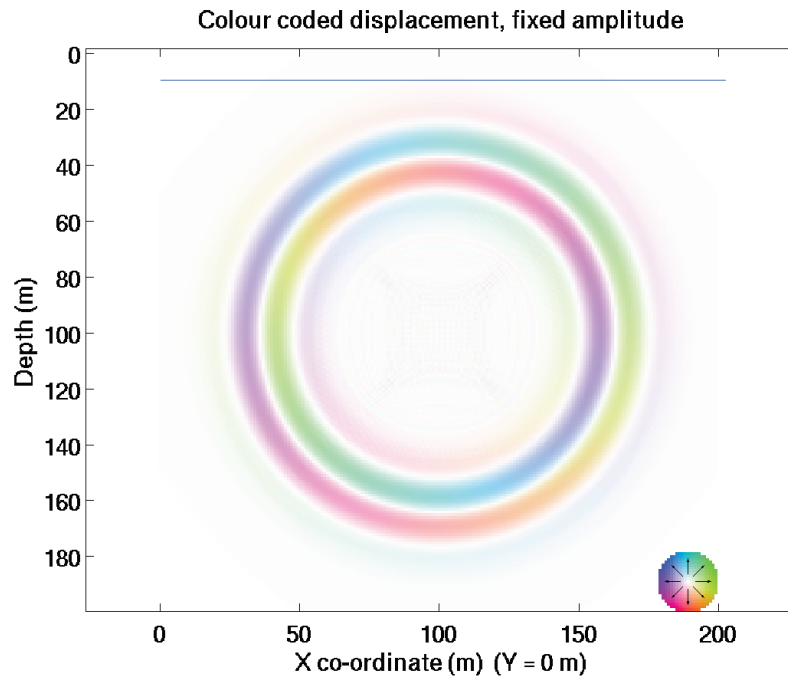
FIG.5. A snapshot from the 'explosive' source. The slice shown here is through the source point, so all displacements are within the plane of the Figure.

Colour coded displacement, fixed amplitude
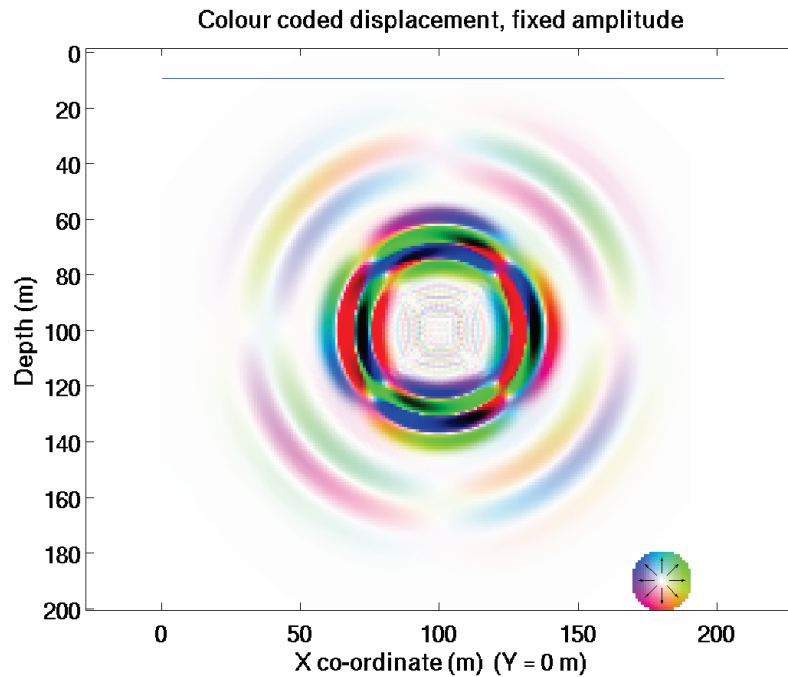
FIG. 6. A snapshot from the 'double couple' source at the same elapsed time as the explosive source in Figure 5. Again, the plane of the Figure is through the source point, but also in the plane of the source vectors. The pressure waves have reached the same distance from the source, but in four quadrants with opposite polarities. The shear waves from the same source travel with half the pressure wave velocity, but their high amplitudes are clipped in this display.
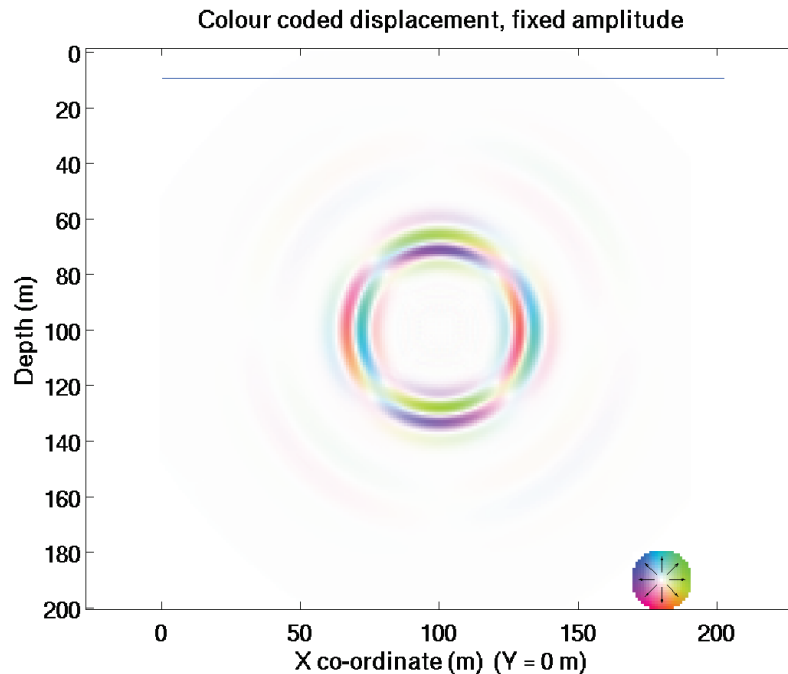

Colour coded displacement, fixed amplitude

FIG. 7. This is a display of the same wavefield as shown in Figure 6, but at a gain level that is reduced by a factor of 9. The colours show shear wave displacement directions, but with the same pattern of alternating polarities shown by the pressure waves. The pattern is oriented at a 45 degree angle from the pressure wave pattern.
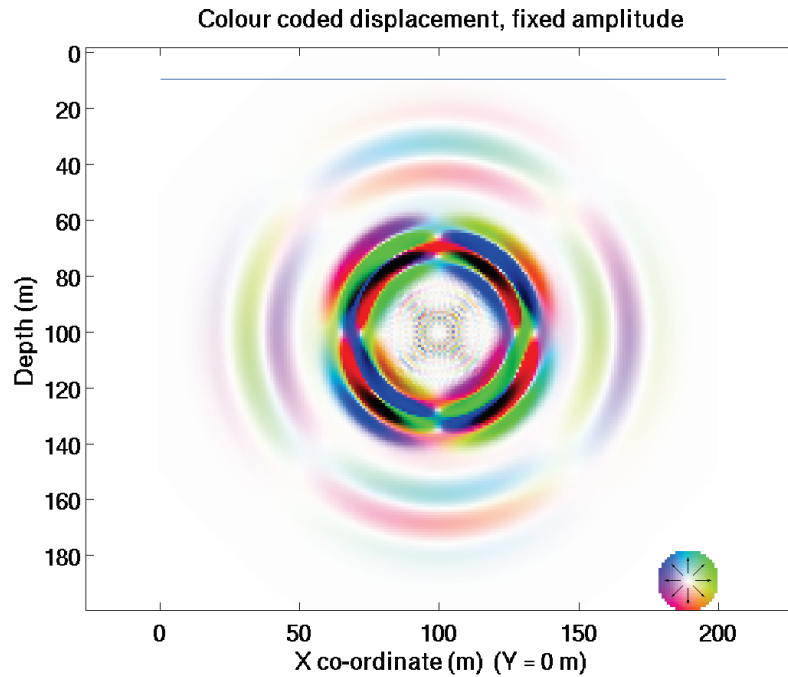
FIG. 8. A snapshot from the 'squeeze/bulge' source, and comparable with the wavefield in Figure 6. The null points are consistent with a rotation between the two figures of 45 degrees.
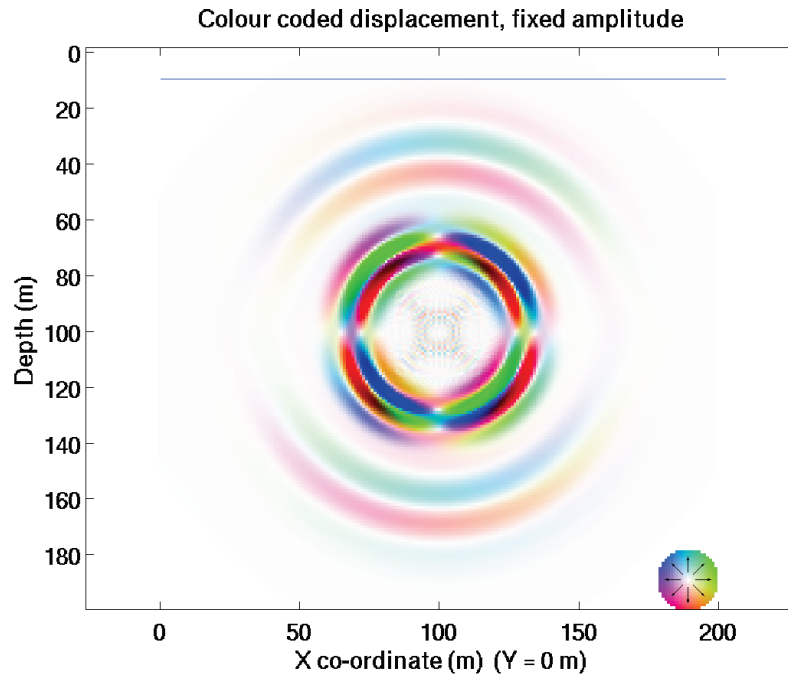

FIG. 9. A snapshot of the wavefield propagated from the 'Z-rupture' energy source. The shear waves here are very similar to those in Figure 8, from the 'squeeze/bulge' source. By contrast, he pressure waves propagate in only two directions, in this case, up and down with null zones at the sides.
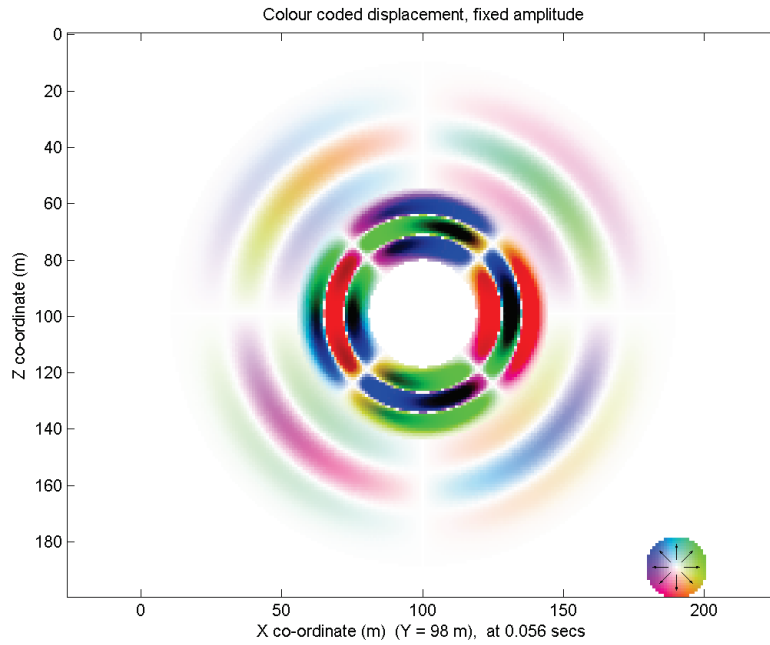
FIG 10. The propagation of the pressure and shear wavefronts from a 'double dipole' source as defined by Aki and Richards, and as predicted by the far-field part of their formulae 4.32 and 4.33. This should be compared with the finite-difference results in Figure 6. The source, a zero phase Ricker wavelet, is obvious here.
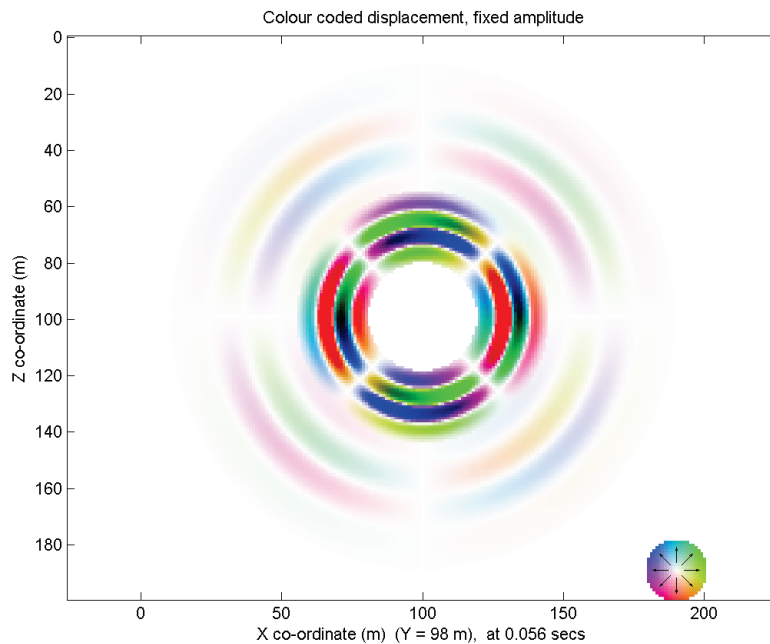

FIG. 11. The wave propagation here is the same as for Figure 10, but the wavelet is the first derivative of the zero phase Ricker wavelet used there. This seems to be a closer match to the finite-difference result in Figure 6.